Water Research 164 (2019) 114869

Contents lists available at ScienceDirect

Water Research

journal homepage: www.elsevier.com/locate/watres

Tracking the contribution of multiple raw and treated wastewater discharges at an urban drinking water supply using near real-time monitoring of β-D-glucuronidase activity

Jean-Baptiste Burnet [a, b, *], Émile Sylvestre [a, b], Jonathan Jalbert [c], Sandra Imbeault [d], Pierre Servais [e], Michèle Prévost [b], Sarah Dorner [a]

[a] Department of Civil, Geological, and Mining Engineering, Polytechnique Montreal, Montreal, Quebec, H3C 3A7, Canada
[b] NSERC Industrial Chair on Drinking Water, Department of Civil, Geological, and Mining Engineering, Polytechnique Montreal, Montreal, Quebec, H3C 3A7, Canada
[c] Département de mathématiques et de génie industriel, Polytechnique Montréal, Montréal, Québec, H3C 3A7, Canada
[d] Service de la Gestion de l'Eau, Ville de Laval, Quebec, H7L 2R3, Canada
[e] Écologie des Systèmes Aquatiques, Université Libre de Bruxelles, Campus de la Plaine, Belgium

ARTICLE INFO

Article history:
Received 24 April 2019
Received in revised form
13 July 2019
Accepted 14 July 2019
Available online 15 July 2019

Keywords:
Escherichia coli
Sewage by-pass
Combined sewer overflows
De facto wastewater reuse
Catchment microbial dynamics
Online monitoring

ABSTRACT

Past waterborne outbreaks have demonstrated that informed vulnerability assessment of drinking water supplies is paramount for the provision of safe drinking water. Although current monitoring frameworks are not designed to account for short-term peak concentrations of fecal microorganisms in source waters, the recent development of online microbial monitoring technologies is expected to fill this knowledge gap. In this study, online near real-time monitoring of β-D-glucuronidase (GLUC) activity was conducted for 1.5 years at an urban drinking water intake impacted by multiple point sources of fecal pollution. Parallel routine and event-based monitoring of *E. coli* and online measurement of physico-chemistry were performed at the intake and their dynamics compared over time. GLUC activity fluctuations ranged from seasonal to hourly time scales. All peak contamination episodes occurred between late fall and early spring following intense rainfall and/or snowmelt. In the absence of rainfall, recurrent daily fluctuations in GLUC activity and culturable *E. coli* were observed at the intake, a pattern otherwise ignored by regulatory monitoring. Cross-correlation analysis of time series retrieved from the drinking water intake and an upstream Water Resource Recovery Facility (WRRF) demonstrated a hydraulic connection between the two sites. Sewage by-passes from the same WRRF were the main drivers of intermittent GLUC activity and *E. coli* peaks at the drinking water intake following intense precipitation and/or snowmelt. Near real-time monitoring of fecal pollution through GLUC activity enabled a thorough characterization of the frequency, duration and amplitude of peak contamination periods at the urban drinking water intake while providing crucial information for the identification of the dominant upstream fecal pollution sources. To the best of our knowledge, this is the first characterization of a hydraulic connection between a WRRF and a downstream drinking water intake across hourly to seasonal timescales using high frequency microbial monitoring data. Ultimately, this should help improve source water protection through catchment mitigation actions, especially in a context of *de facto* wastewater reuse.

1. Introduction

Safe water supply is essential for human health and sustainable growth. At a global scale, treated surface water (from rivers, lakes, reservoirs) accounts for at least 50% of the drinking water needs (IWA, 2019). Yet, most of these supplies are affected by fecal pollution, and their integrity is increasingly threatened by growing

* Corresponding author. Department of Civil, Geological, and Mining Engineering, Polytechnique Montreal, Montreal, Quebec, H3C 3A7, Canada.
E-mail address: jean-baptiste.burnet@polymtl.ca (J.-B. Burnet).

https://doi.org/10.1016/j.watres.2019.114869
0043-1354/

populations, urbanization and climate change (Khan et al., 2015; WHO, 2017). Consequently, unplanned (*de facto*) wastewater reuse through abstraction of surface water impacted by treated and/or untreated wastewater for drinking water production has become common practice worldwide (Drewes et al., 2017; Rice et al., 2013). Intense precipitation and snowmelt episodes can substantially deteriorate the microbiological quality of source waters as they trigger the release of untreated sewage into the receiving drinking water supplies through combined sewer overflows (CSOs) and/or Water Resource Recovery Facilities' (WRRFs) by-passes (Madoux-Humery et al., 2016; Tolouei et al., 2019; Tornevi et al., 2014; Young et al., 2015). In developed countries, large waterborne outbreaks have mainly occurred following extreme water-related weather events (Cann et al., 2013; Curriero et al., 2001). CSOs and wastewater bypasses typically discharge over the course of a few hours, but they can generate rapid short-term increases in fecal contaminant concentrations in rivers (Jalliffier-Verne et al., 2016; Madoux-Humery et al., 2015; Ouattara et al., 2014; Weyrauch et al., 2010). Identifying peak contamination periods and understanding the occurrence, fate and transport of fecal contaminants upstream of water abstraction sites is therefore crucial for prioritizing actions towards mitigation of fecal pollution sources and human health protection (WHO, 2016). This need becomes even more urgent as the vulnerability of drinking water sources to fecal pollution is expected to grow with global changes (Jalliffier-Verne et al., 2017; WHO, 2017).

Current monitoring practices for source waters (monthly to weekly, daily sampling at best) are not suited for reliable identification of hazardous events, as infrequent manual sampling easily misses episodic contamination spikes (Madrid and Zayas, 2007; Signor and Ashbolt, 2006; Stadler et al., 2008). This is due to the highly fluctuating nature of microbial temporal dynamics in water (Boehm, 2007; Burnet et al., 2014) but also to methodological limitations of standard assays, which rely on culture-based enumeration of FIB that require at least 24 h-incubation periods. Madoux-Humery et al. (2016) demonstrated the limitations of current methodologies for reliable identification and characterization of peak *E. coli* concentrations in drinking water supplies impacted by intermittent CSOs, advocating for the need of online monitoring.

Rapid and high-frequency monitoring of microbial water quality therefore represents a crucial step towards efficient identification and management of hazardous events in drinking water supplies. In recent years, online technologies capable of measuring microbial parameters at high frequency (<hourly) have been developed and successfully implemented in various field settings, from source to the tap (IWA, 2018). These technologies include flow cytometry (Besmer et al., 2014; Page et al., 2017), enzymatic activity (Ender et al., 2017; Ryzinska-Paier et al., 2014; Stadler et al., 2016; Tryland et al., 2015) as well as optical and humic acid-like fluorescence (Højris et al., 2016; Sorensen et al., 2015). Enzyme-based assays specifically quantify the occurrence of fecal indicator bacteria (FIB) such as *E. coli* by targeting metabolic enzymes already in use in conventional culture-based assays for these bacteria. In the case of *E. coli*, the activity of β-D-glucuronidase (GLUC) enzyme is predominantly correlated to the occurrence of *E. coli* in water (Farnleitner et al., 2001; Fiksdal et al., 1994; Garcia-Armisen et al., 2005) although cross-reactions with other (fecal) bacteria exist (Fiksdal and Tryland, 2008). Recent studies have demonstrated that online GLUC activity monitoring provided an unprecedented wealth of information on the temporal dynamics of microbial water quality in various habitats and that GLUC activity could represent a valuable early warning tool for fecal pollution of water resources (Burnet et al., 2019; Ender et al., 2017; Ryzinska-Paier et al., 2014; Stadler et al., 2016, Stadler et al., 2019a). Also, Stadler et al. (2019b) demonstrated how automated GLUC activity monitoring contributed to understanding the sources and pathways of fecal pollution in an agricultural headwater catchment. Most studies on the use of online GLUC activity as biochemical surrogate of fecal pollution have not been conducted in the context of drinking water supply. Yet, near real-time monitoring of microbial water quality could provide valuable knowledge on the sources and pathways in these environments and improve water quality assessment and management.

The objectives of the present study were therefore to gain new insights into the sources and processes driving microbial water quality in an urban drinking water supply using near real-time monitoring of GLUC activity for more than 1.5 years. First, we sought to unravel the temporal scales of variation in GLUC activity and explicitly characterize peak contamination events. Secondly, we contextualized the short- and long-term GLUC activity trends using available online physico-chemistry as well as hydrometeorological and sewershed data, in order to understand the drivers of the temporal patterns in microbiological water quality. Thirdly, we investigated the relationships between GLUC activity and culturable *E. coli* as well as online physico-chemical parameters through routine and event-based sampling to evaluate the benefit of online microbial monitoring. We finally propose an optimized strategy for targeted collection of microbial water quality data using online monitoring of GLUC activity. To the best of our knowledge, this is the first study using high frequency microbial monitoring in water supplies for the identification of fecal contaminant sources.

2. Material and methods

2.1. Site description

The studied drinking water treatment plant (DWTP) draws water from a 42-km long river located in the Greater Montreal Area, in southwestern Quebec, Canada. The river originates from the St-Lawrence-Ottawa river system and feeds four additional DWTPs, which serve >556,000 people in total. The surrounding catchment adjacent to the river is predominantly characterized by urban land use, with a total of 9 water resources recovery facilities (WRRFs) and 190 combined sewer overflows (CSOs) discharging (un)treated wastewater intermittently to the river. Among these, 4 WRRFs and 37 CSO outfalls are located upstream the studied DWTP intake (3 WRRFs and 30 CSO outfalls occur within the intermediate protection zone of the intake) (Fig. 1). Intermediate protection areas of drinking water intakes encompass a 10-km river stretch upstream from the intake (MDDELCC, 2016). Although agricultural land is limited in the investigated area, additional diffuse sources of *E. coli* could contribute to the faecal pollution load at the DWTP intake. Based on 26 years of data (1981–2016), the annual average river flowrate ranges from 140 to 315 $m^3 s^{-1}$ and flowrates are highest in April and May and lowest from July to September (monthly averages ranging between 380 and 468 $m^3 s^{-1}$ and between 144 and 177 $m^3 s^{-1}$, respectively) (Environment Canada, 2019).

2.2. Sampling strategy

Samples were collected routinely (three days per week between Monday and Thursday) and analyzed for *E. coli* concentrations by the DWTP staff over the study period (November 2016 to May 2018). Additional high frequency sampling was conducted for 24–48 h using an ISCO 6712 autosampler (Teledyne) in parallel to online monitoring of GLUC activity. These campaigns were performed under dry weather conditions (absence of rainfall or snowmelt 72 h prior sampling) and during contamination events following rainfall/snowmelt episodes. Collected samples were

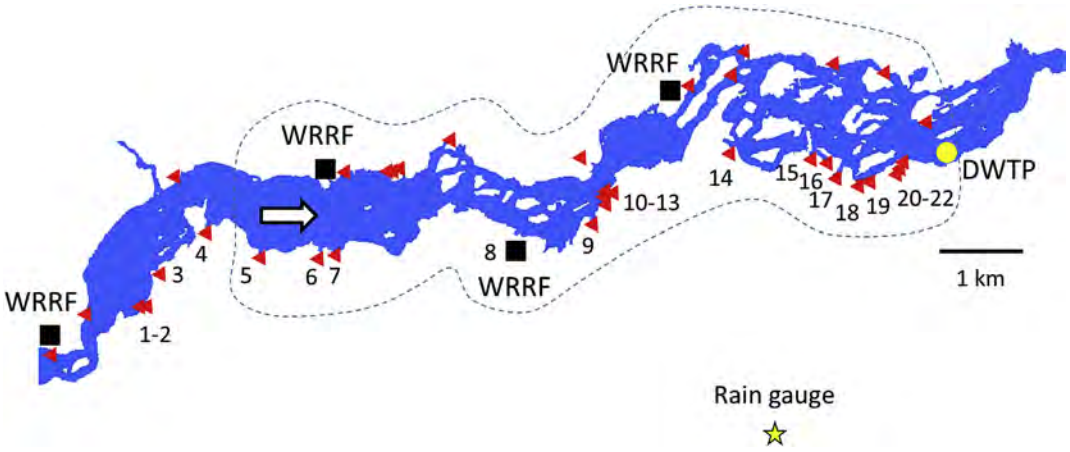

Fig. 1. Map of the study area including the drinking water treatment plant (DWTP) intake (yellow dot), water resources recovery facilities (WRRF) (black squares) and combined sewer overflow (CSO) outfalls (red triangles). In this study, only CSO outfalls (1–7, 9–22) and the by-pass of a WRRF (8) located on the south riverbank were investigated. The white arrow indicates flow direction and the intermediate protection zone of the intake is delimitated by the dashed line. (For interpretation of the references to color in this figure legend, the reader is referred to the Web version of this article.)

selected at (bi-)hourly frequency along the GLUC activity pollutograph for further enumeration of culturable *E. coli*. Online GLUC activity measurements do not involve a pre-filtration step as for the manual assay (Garcia-Armisen et al., 2005), therefore we tested for possible soluble interferents that could contribute to the total GLUC activity signal (Fiksdal and Tryland, 2008). In March 2018, six additional samples (one sample every 4 h) were filtered through a sterile 47-mm, 0.22 μm pore size mixed cellulose ester membrane filter (Millipore) for the measurement of GLUC activity in the soluble (<0.22 μm) fraction of the sample. In a subset of collected samples (1 sample every 6 h), culturable *E. coli* were also enumerated in triplicate to determine the analytical variability associated with the culture-based assay. The analytical variability of GLUC activity measurements was low, not exceeding 5% on average (Burnet et al., 2019).

2.3. Culture-based enumeration of E. coli

Enumeration of culturable *E. coli* during routine and event-based monitoring was performed by membrane filtration using USEPA method 1604 (USEPA, 2002). During three additional high-frequency sampling campaigns, temporal fluctuations in *E. coli* concentrations were assessed using defined substrate technology (Colilert Quanti-Tray/2000, IDEXX) by following the instructions of the manufacturer. Previous investigations showed that USEPA 1604 and Colilert assay were highly correlated ($r > 0.9$) (Burnet et al., 2019).

2.4. Online monitoring of β-D-glucuronidase (GLUC) activity

Near real-time monitoring of β-D-glucuronidase (GLUC) activity was performed with a ColiMinder Industrial instrument (VWM Solutions GmbH) at the raw water from November 2016 to May 2018. The analytical validation of the technology (precision and robustness) has been recently completed within the study area (Burnet et al., 2019). The instrument was continuously supplied with raw water from the same pipe used for turbidity, conductivity and temperature online monitoring. Measurement frequency was set at bi-hourly frequency (12 measurements per day) or hourly frequency during selected peak contamination events. Raw data were continuously recorded, transmitted via a wireless modem and accessed/downloaded remotely.

The rate of fluorescence emitted during the enzymatic reaction in the flow-through photometric measurement chamber of the device was expressed in volts per second and converted into Modified Fishman Units per 100 mL (MFU.100 mL^{-1}). Calibration by the manufacturer used commercial enzyme standards (G7396-25KU, type IX-A β-D-glucuronidase from *E. coli*, Sigma-Aldrich) with further details provided by Koschelnik et al. (2015). As determined by the manufacturer, the limit of quantification (defined as the reproducible signal exceeding background noise) was 0.8 mMFU.100 mL^{-1}.

Since the measurement process itself is based on light intensity measurements of fluorescence, transmission and reference light intensity, calibration of instrument sensors and amplification as well as checking of measurement chamber cleanliness was automatically performed every 25 measurements. Light calibration was intended for removal of any long-term effects of changing sensor properties or possible build-up of scale on the glass of the measurement chamber. The temperature in the measurement chamber was continuously controlled and recorded.

Reagents and buffers were stored as recommended by the manufacturer. The fluorogenic substrate (CM.EC QuickDetect Reagent A. VWM Solutions GmbH) and buffer (CM.EC QuickDetect Reagent B, VWM Solutions GmbH) were stored at −20 °C and 4 °C, respectively, before use. During the deployment phase as well as during laboratory experiments, both solutions were maintained at 4 °C in the cooling block of the instruments. Reagent quality was ensured by VWMs Quality Control process using defined enzyme calibration solutions. Reagent dosage in the device was verified through blank tests, which were automatically carried out with Milli-Q water after 24 measurements to correct for any offset in GLUC activity measurements. The GLUC activity measured during blank tests (assay buffer + assay substrate + Milli-Q water) was automatically deducted from the measurement results of raw water samples to eliminate a possible influence of substrate quality and aging (ex. autohydrolysis of the reagent).

2.5. Hydrometeorology and online physico-chemistry

Raw water turbidity (Surface Scatter sc turbidimeter, HACH), conductivity, temperature and pH (sc100, HACH) were measured online at the intake and operated by the DWTP staff. Flow rate data were extracted from the public repository of Environment Canada (Environment Canada, 2019). Daily rainfall data was obtained from the municipal partner for the closest rain gauge (Fig. 1).

2.6. Combined sewer overflows, WRRF by-passes and treated effluent discharges

Sewershed data were provided by the partner municipality. Location, duration and frequency were gathered (whenever available) for each combined sewer overflow (CSO) outfall located upstream from the drinking water intake. As complete transversal mixing should occur within a distance equal to 100–1,000 river widths (Jirka et al., 2004), and given the proximity of upstream pollution sources to the drinking water intake within the investigated stretch of the river, only those discharge points located on the same riverbank were suspected of impacting the DWTP intake (Fig. 1). Continuously measured process data (online flow rate in raw sewage and UV fluence applied to effluents) were obtained for the WRRF located 6 km upstream from the drinking water intake. The treatment at this WRRF includes degritting and settling followed by UV disinfection of the primary effluent. The residence time in the WRRF averages 2.5 h (for an average flow rate of 51,600 $m^3.day^{-1}$ during the study period) but it can drop to 1.5 h during peak flow rates of 75,000 $m^3.day^{-1}$ (G. Filiatrault, *personal communication*). Additional information on the frequency, duration and volumes of the sewage by-passes recorded at the WRRF during the study period was obtained from the municipality.

2.7. Statistical analyses

Cross-correlation and linear regression analyses were performed to investigate the dependency between time series for the parameters measured during the study period.

Cross-correlation analysis was performed to assess the lag time between time series at the WRRF and at the downstream DWTP. For the WRRF, discharge rates were only available for the plant inlet (raw sewage) but were considered representative of treated effluent discharge rates. For the DTWP intake, online GLUC activity measurements were used. Considering the seasonal patterns of GLUC activity, these analyses were conducted for two separate periods of the year. The first period, referred to as "high GLUC activity" encompassed 8 months between fall and early spring (after the last snowmelt) while the second period, referred to as "low GLUC activity" spanned over the remaining 4 months. The time lag between the WRRF effluent and the downstream DWTP intake depends both on the discharge rate in the WRRF and the river flow rate. As both time series (discharge rate in raw sewage and GLUC activity at downstream DWTP) did not possess the same measurement frequency, they were linearly interpolated for a common temporal x axis. Correlation analysis (Chatfield, 2003) between the variables were then performed using the linear correlation coefficient and linear regression analysis. The cross-correlation measured the similarity of the first time series and the shifted copies of the second one and the delay between measurements was estimated by selecting the highest cross-correlation coefficient (0.94 and 0.84 for "high GLUC activity" and "low GLUC activity" datasets, respectively).

Linear regression analyses were performed between GLUC activity, online physico-chemistry, *E. coli*, river flow rate and WRRF discharge rate for the GLUC activity periods as defined above. Estimated lag times between WRRF effluent and DWTP intake were integrated into regression analyses. All statistical analyses were performed in Matlab (Mathworks).

3. Results

3.1. Hydrometeorological conditions

Fig. 2 shows the hydrological and meteorological conditions of the investigated area from November 17, 2016 to May 31, 2018. In comparison to historical measurements, the study period was characterized by higher-than-average precipitation (Fig. S3a). Monthly rainfall exceeded the monthly averages (1981–2010) for 14 out of the 19 months of the study. This trend was particularly pronounced from January to May 2017, during which monthly rainfall accumulation was 1.5–3.2-fold higher than the 30-year averages. The rainiest month of the study was April 2017 (169.7 mm) and highest daily precipitation was recorded on May 1, 2017 (58.1 mm). The monthly mean snow cover observed during the study ranged between 1 cm (November 2017) and 15 cm (February 2018), and was similar to the monthly mean cover (30-year average) (Fig. S3b). Highest daily flow rates were recorded in May 2017 (1080 $m^3 s^{-1}$), following cumulative snowmelt and rainfall episodes that resulted in the 2017 spring flood in the Greater Montreal Area. During and following this spring flood, monthly flow rates from May 2017 to July 2017 exceeded historical (1981–2016) monthly averages by 1.4–2.4 times (Fig. S3c). Lowest monthly flow rates were measured in November 2016 (83 $m^3 s^{-1}$).

3.2. Near real-time monitoring of β-D-glucuronidase activity at the drinking water intake

High frequency monitoring of GLUC activity yielded a total of 5,992 measurements. In addition, a total of 223 blank measurements were carried out by the device and generated average GLUC activities of 0.7 ± 1.3 mMFU.100 mL^{-1} which were automatically deducted from raw water GLUC activity. The latter ranged from 2.2 to 56.6 mMFU.100 mL^{-1} with an average of 11.3 mMFU.100 mL^{-1} and a 95th percentile of 27.7 mMFU.100 mL^{-1}. The "high GLUC activity" and "low GLUC activity" periods displayed an average GLUC activity of 15.2 ± 7.5 mMFU.100 mL^{-1} ($n = 3,895$) and 5.3 ± 2.1 mMFU.100 mL^{-1} ($n = 2,097$), respectively. GLUC activities exceeding the 95th percentile value (defined here as peaks) occurred during 15 time periods over the 1.5 years. These GLUC activity peaks lasted on average 36 h but could be observed for up to 10 days. The longest GLUC activity peak episodes occurred following snowmelt events (Fig. 2).

GLUC activity medians were 2 to >4 times lower in summer compared to the other seasons (Fig. S2). The variability in GLUC activities was also lower during summer months compared to the rest of the year. Daily patterns were recurrently observed at the intake; GLUC activity increased overnight before decreasing during the day (Fig. 3a). Almost 75% of GLUC activity daily maxima occurred between 10 p.m. and 7 a.m. (Fig. 3b). In the absence of rainfall or snowmelt events, the amplitude of these daily fluctuations increased from ~2 mMFU.100 mL^{-1} in summer to ~5 mMFU.100 mL^{-1} between fall and spring (Figs. 4–5, Figs. S4–S5). Measurements of GLUC activity in the soluble (<0.22 μm) fraction (representing the extracellular GLUC activity and/or soluble interferents) displayed a stable background signal of 2.4 mMFU.100 mL^{-1}, which constituted 15% of the total GLUC activity signal (Fig. 3a).

3.3. Routine and event-based monitoring of Escherichia coli at the drinking water intake

The 1.5-year routine monitoring of *E. coli* at the intake (3 days a week, $n = 220$ samples in total) yielded a mean concentration of 132 CFU.100 mL^{-1} (min. 1 to max. 1,100 CFU.100 mL^{-1}, 95th percentile of 410 CFU.100 mL^{-1}) and a median concentration of 80 CFU.100 mL^{-1}. The seasonal pattern of *E. coli* concentrations was less pronounced than that observed for GLUC activity (Fig. S2).

During event-based sampling in February, March and April 2017, a total of 65 samples were collected along the pollutographs (as

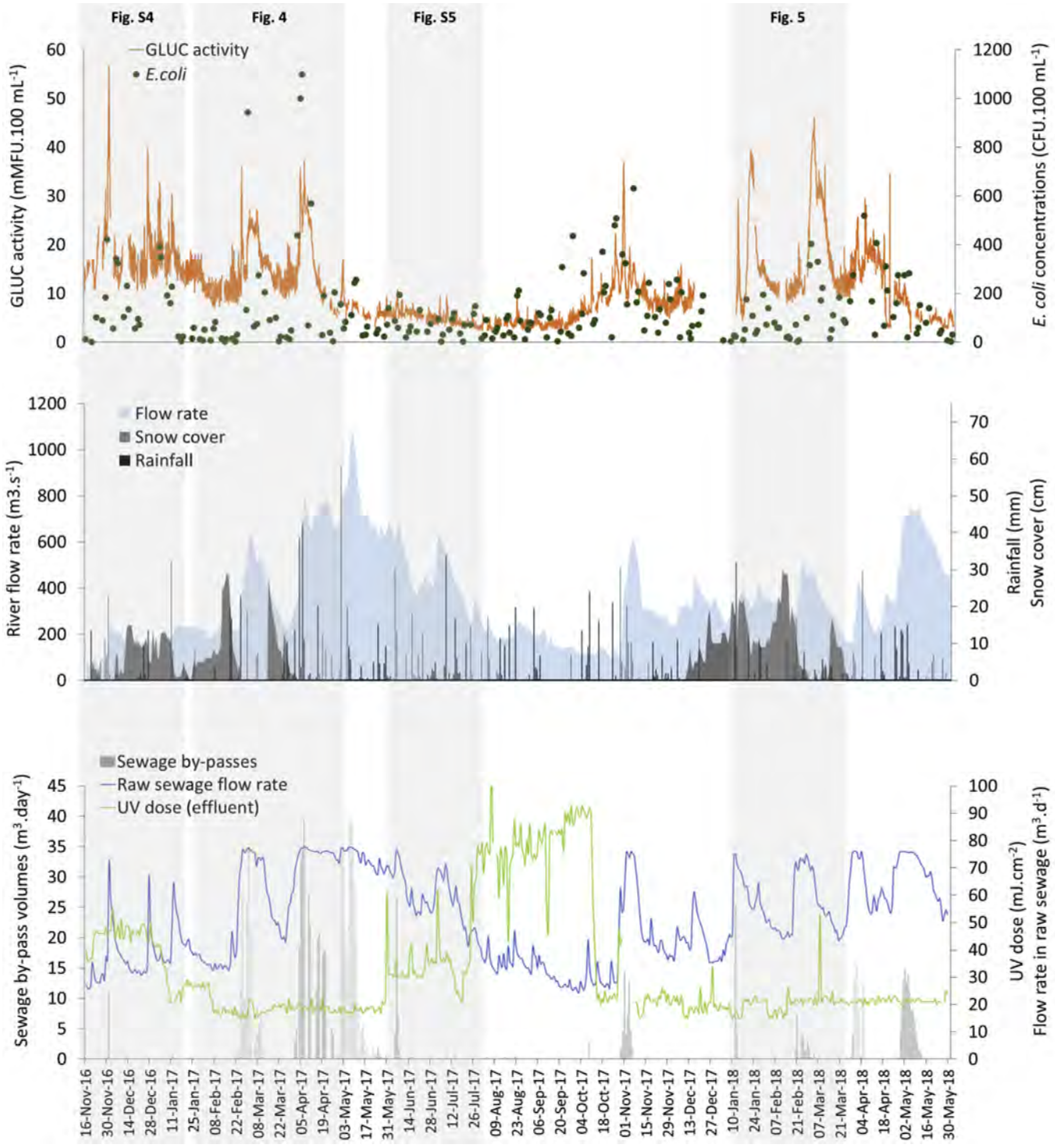

Fig. 2. Time series (from Nov 2016 to May 2018) of GLUC activity (min. 12 measurements per day) and concentrations of culturable *E. coli* (1 measurement per day, 3 days a week) at the drinking water intake in relationship with local hydrometeorology and wastewater discharges from a WRRF located 6 km upstream and on the same riverbank (outfall #8, Fig. 1). Shaded areas are detailed in Figs. 4–7.

defined by hourly GLUC activity measurements) and maximal *E. coli* concentrations reached 2,720 CFU.100 mL^{-1}. During the three event-based sampling campaigns, peak *E. coli* concentrations were synchronous with peak GLUC activities (Fig. 4).

3.4. Treated wastewater discharges, by-passes and combined sewer overflows

The WRRF located 6 km upstream from the drinking water

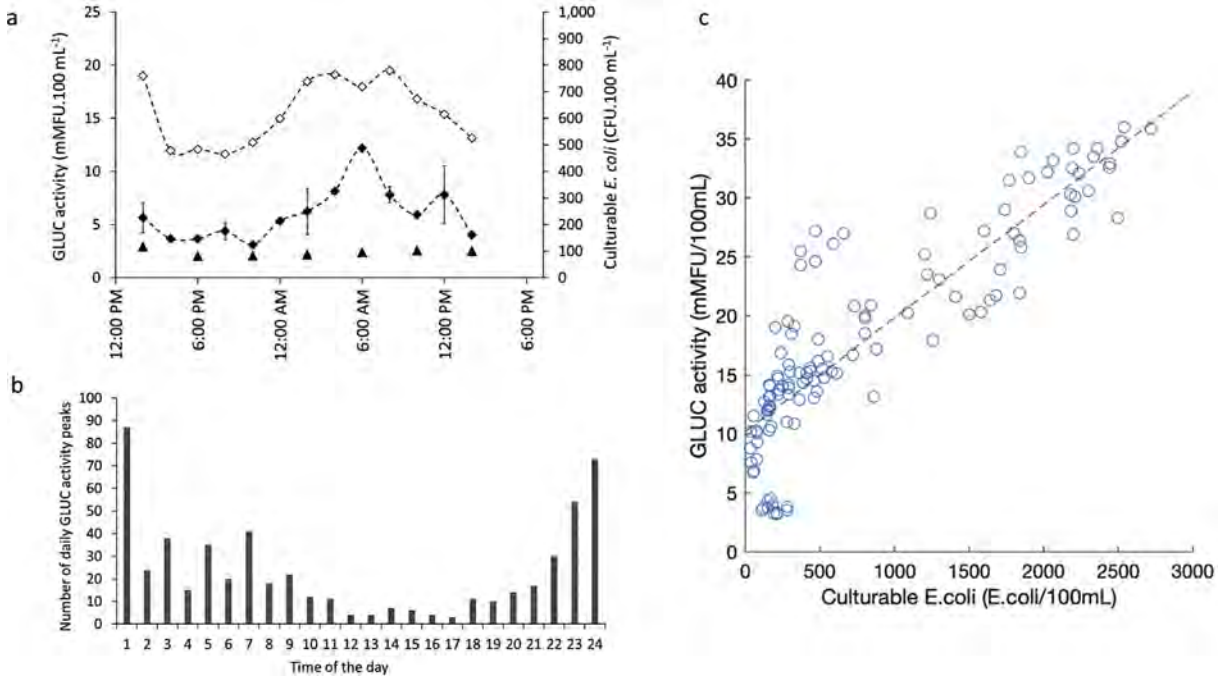

Fig. 3. Daily fluctuations of GLUC activity at the drinking water intake, a) 24-h dynamics of GLUC activity (open circles), soluble GLUC activity (black triangles) and culturable *E. coli* concentrations (black dots) under baseline conditions (absence of rainfall 3 days prior sampling) in March 2018. Culturable *E. coli* were enumerated in triplicate every 6 h (coefficients of variation from 10 to 35%). b) frequency of the timing at which daily peak GLUC activities were measured at the intake over the 1.5-year period, c) linear regression between GLUC activity and *E. coli* during daily fluctuations under baseline and event conditions (data pooled from 8 high frequency sampling campaigns, $R^2 = 0.76$, $p < 0.001$, $n = 121$).

intake (Fig. 1) released effluents that were UV-disinfected all year round, but the fluence varied seasonally and was highest from the end of July to early October (Fig. 2). Untreated sewage (degritting only) was released into the river during by-pass events recorded for 148 days (out of 561 days). Snowmelt and rainfall accounted for >95% of these by-passes, while only 5% occurred during dry weather. Daily by-pass volumes caused by rainfall and/or snowmelt ranged from 27 to 39,848 m^3 (average of 8,582 m^3) and were higher compared to dry weather by-pass events (17–1,877 m^3, average of 691 m^3). A significant ($p < 0.001$) cross-correlation was found between the flow rate at the WRRF and the GLUC activity measured at the downstream DWTP intake (Fig. 6).

For CSO discharges located within the intermediate protection area of the intake (i.e. outfalls 5 to 22, Fig. 1), half of them discharged over the study period, accounting for 58% of the discharge events for all 22 CSOs located on the south riverbank (Fig. S1). Among them, outfalls 5–7 were the most active, accounting for almost 65% of the CSO events recorded within the intermediate protection area. They were followed by CSO no. 17 (21%), which is one of the closest discharge points (<2 km) upstream from the intake (Fig. 1). Volumes discharged by the different CSOs were not available. Approximate volumes were estimated by the municipality for the discharge points closest to the intake and they did not exceed 20 m^3 for a five-year recurrence modified Chicago-type rainfall episode of 3 h (L. Autixier, *personal communication*).

Time delays between the WRRF and the DWTP measurements were estimated for two different periods: winter and summer. In winter, the cross-correlation analysis was performed on data from Feb 1 to Feb 23, 2017. This period was selected to isolate the baseline signals in absence of rainfall/snowmelt. The similarity between the signals from the WRRF and DWTP was maximal for a 4-h time lag, representing the time for the water to travel from the WRRF inlet to the DWTP intake. In summer, the cross-correlation analysis was performed on data from July 1 to August 8, 2017. The similarity between the two signals was maximal for a time lag of 8.5 h.

3.5. Correlations between GLUC activity and online physico-chemical parameters at the intake

Relationships between GLUC activity and online physico-chemical parameters were assessed for two different periods of the year characterized by either “high” or “low” GLUC activities (as defined in section 2.7) and which encompassed fall to early spring and late spring to summer months, respectively. Colored boxes of the correlation matrices (Fig. 7) are significant at the level of $\alpha = 1/1000$. Blank boxes indicate the absence of significant relationships at the level of $\alpha = 1/20$. GLUC activity was significantly correlated with culturable *E. coli*, turbidity, conductivity as well as river and raw sewage flow rates although the strength of the relationships varied among parameters and between “low GLUC activity” and “high GLUC activity” periods.

4. Discussion

4.1. Impact of the continuous upstream release of treated effluents on the microbial water quality at the drinking water intake

A recurrent daily pattern in GLUC activity was observed throughout the year at the intake of the drinking water treatment plant (Figs. 4–5, Figs. S4–S5). The overall trend consisted in an increase of GLUC activity in the evening, followed by an overnight peak and a gradual decrease over the day (Fig. 3). In a previous study, Stadler et al. (2016) also reported daily GLUC activity fluctuations in a small agricultural catchment, but the daily peaks occurred in the late afternoon and were apparently not associated with sewage discharges. In a karst spring in Vietnam, Ender et al. (2017) observed GLUC activity peaks in the evening and

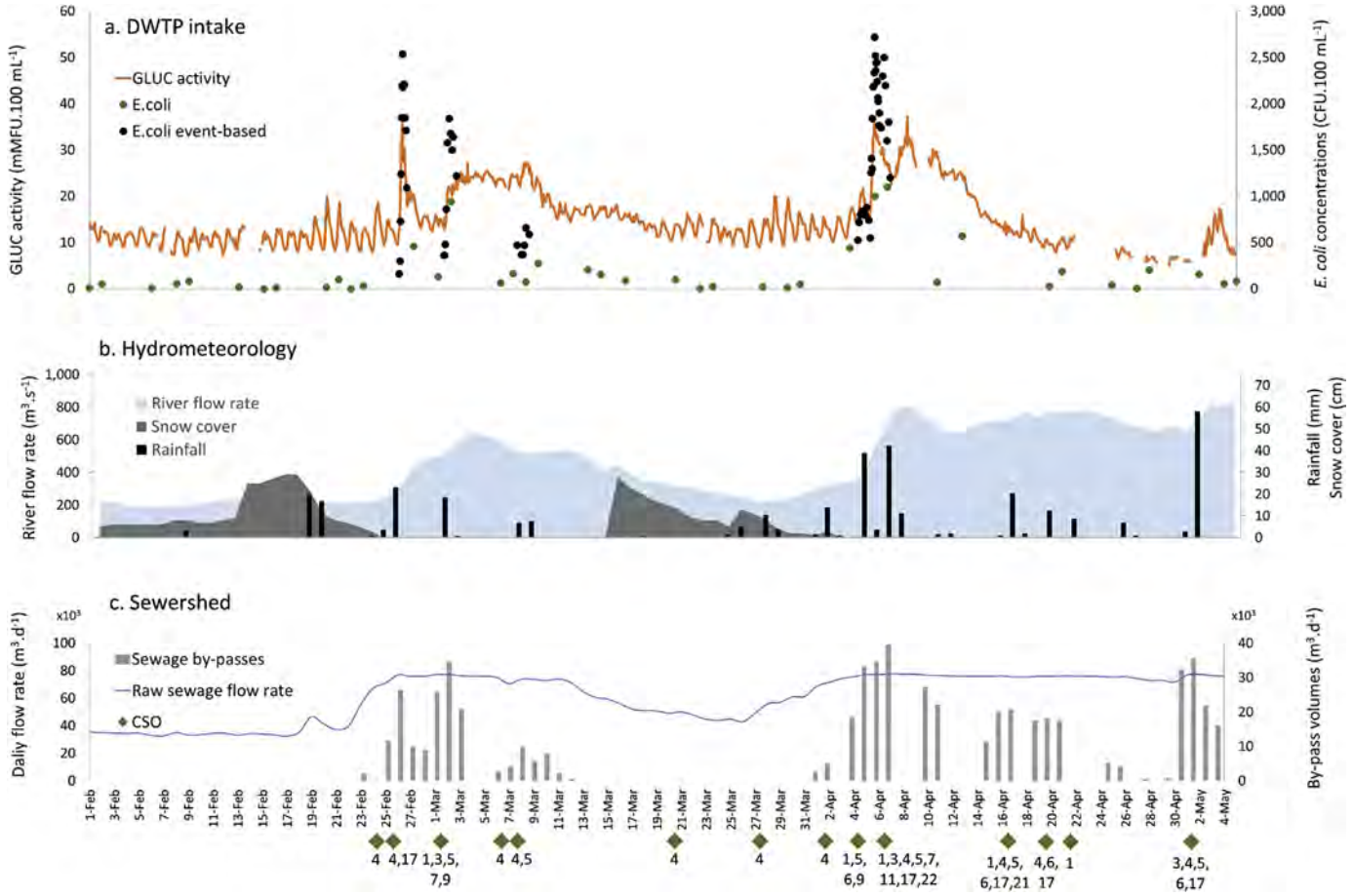

Fig. 4. Impact of the release of treated, untreated, or partially treated sewage on the fecal pollution dynamics at the intake of the drinking water treatment plant during combined snowmelt/rainfall-induced runoff events in February, March and April 2017. Near real-time GLUC activity measurements were combined with routine and event-based monitoring of *E. coli* (green and black circles, respectively). The number associated with combined sewer overflow events (CSO) refers to the outfalls identified in Fig. 1. MFU, modified Fishman units; CFU, colony-forming units. (For interpretation of the references to color in this figure legend, the reader is referred to the Web version of this article.)

suspected anthropogenic activities in the recharge area of the spring to cause these spikes. However, their observations were based on a limited set of data and the drivers of these daily fluctuations were not explicitly identified.

In this study, the amplitudes of daily GLUC activity fluctuations under baseline conditions varied between seasons. Highest amplitudes were observed from late fall to early spring, and lowest in summer (Figs. S4–S5). For a 1-month period representative of winter conditions (mid-January to mid-February 2017), the amplitude averaged 4.7 ± 1.1 mMFU.100 mL^{-1}. During that same period, the amplitude of daily water temperature fluctuations averaged 0.1 ± 0.2 °C, which minimizes the importance of any temperature-related processes affecting enzymatic activity (Bergmeyer, 2012). The low and stable GLUC activity signal measured in the soluble fraction of intake samples (Fig. 3a) leaves out the possibility of measurement interferences by extracellular GLUC activity or non-target compounds (Fiksdal and Tryland, 2008). Instead, concentrations of culturable *E. coli* displayed similar daily patterns and were significantly correlated to GLUC activity (Fig. 3). The hypothesis of a unique and continuous discharge inducing daily microbial water quality fluctuations of river water at the intake was eventually confirmed by cross-correlation analysis (Fig. 6). The latter revealed a strong ($p < 0.001$) association between the GLUC activity time series measured at the intake and the lagged time series for sewage discharge rate at a WRRF located 6 km upstream of the intake. This link was more pronounced in winter than in summer, as rainfall episodes and resulting increases in treated effluent discharge rates generated higher amplitudes of daily GLUC activity fluctuations (Fig. 4, Fig. S4). Daily fluctuation patterns disappeared or were strongly attenuated following major snowmelt runoff episodes, illustrating the overlapping drivers of GLUC activity dynamics in the catchment. (Fig. 5). Numerous studies have documented the impact of WRRF effluents on the chemical and microbiological quality of receiving waters (Jalliffier-Verne et al., 2016; Madoux-Humery et al., 2016; Ort and Siegrist, 2009; Ouattara et al., 2014). To the best of our knowledge though, this is the first time that the hydraulic connection between a WRRF and a downstream DWTP is characterized across hourly to seasonal scales using high frequency microbial monitoring data.

4.2. Impact of intermittent releases of untreated sewage on the microbial water quality at the drinking water intake

In addition to the continuous release of treated effluents, the WRRF discharged partially treated sewage (after degritting) into the river at 148 occasions during the study period, which triggered major GLUC activity peaks (Fig. 2). Sewage by-passes occurred when the daily capacity of the WRRF (75,000 m^3.day^{-1}) was surpassed, usually following snowmelt and/or intense precipitation episodes. During the combined rainfall-snowmelt episodes of February and April 2017, discharged sewage volumes exceeded

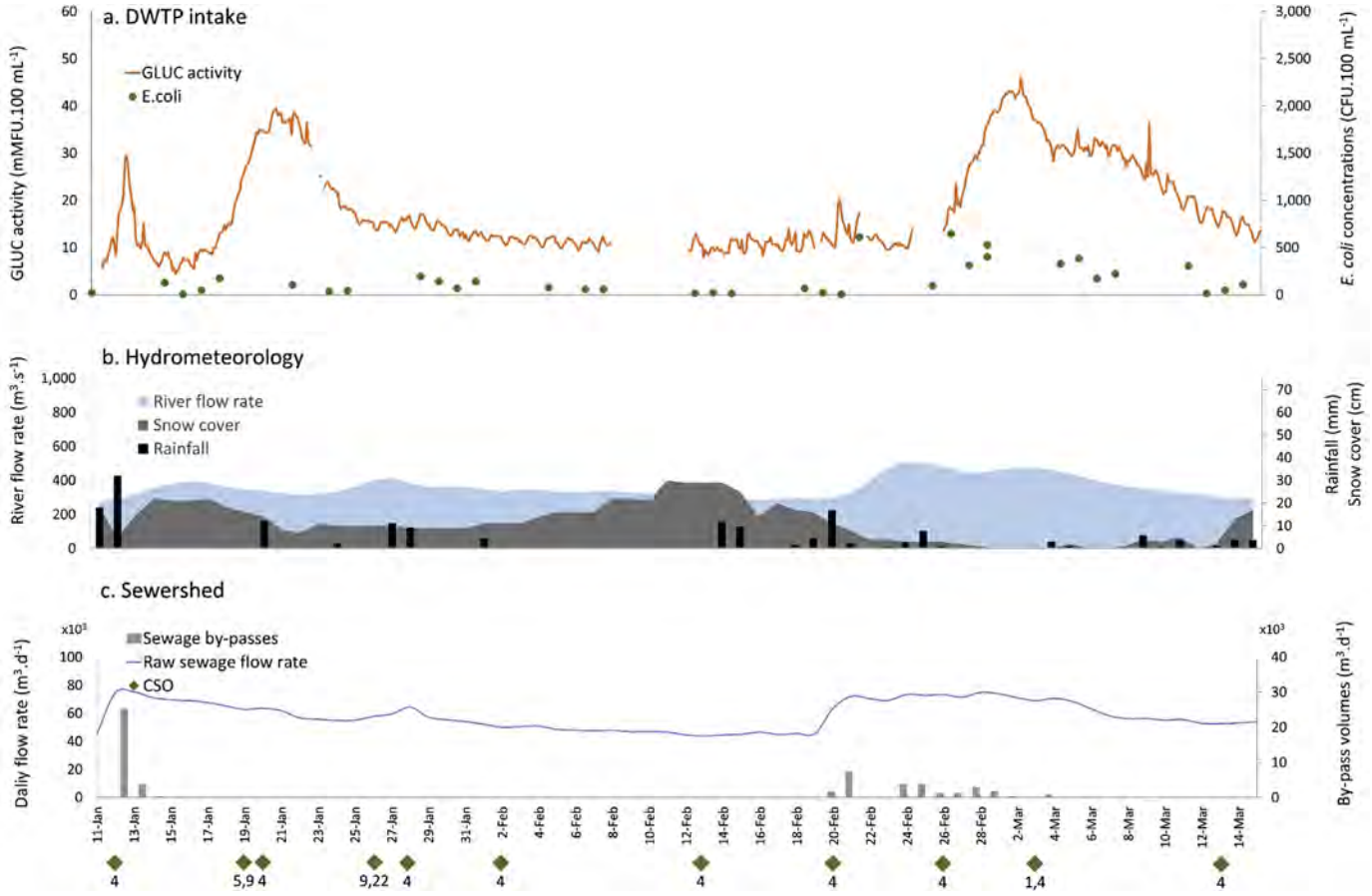

Fig. 5. Short-term dynamics of GLUC activity (orange line) and *E. coli* (green circles for routine monitoring) in relationship with local hydrometeorology and an upstream WRRF (flow rate at WRRF inlet and sewage by-passes) in January and March 2018. MFU, modified Fishman units; CFU, colony-forming units. (For interpretation of the references to color in this figure legend, the reader is referred to the Web version of this article.)

30,000 $m^3.day^{-1}$ on several occasions, which was reflected by rapid increases in GLUC activity and culturable *E. coli* at the downstream DWTP intake (Fig. 4).

Additional releases of raw sewage by combined sewer overflows (CSOs) were also observed (Figs. 4–5, S4-S5). Most CSO events were recorded for outfall #4 (Fig. 1, Fig. S1), but the latter did not appear to affect GLUC activity dynamics, likely because of its distance (11 km) to the intake. In addition, estimated discharge volumes for the closest CSO outfalls #17 and #20–22 (L. Autixier, *personal communication*) were on average more than 500-fold lower than those of sewage by-passes at the WRRF. Although the low number of CSOs equipped with online recorders hampered the precise assessment of their relative contribution to *E. coli* loads at the intake, their impact is expected to be limited compared to the WRRF by-passes. Results from the investigated urban catchment thus underscore the predominant influence of WRRF by-passes on the microbial water quality at the intake, especially during winter and spring.

4.3. Local hydrometeorology governs GLUC activity short and long-term dynamics

The seasonality of microbial parameters in water is associated with catchment-specific and hydrometeorological-driven processes (Wilkes et al., 2009). In our study, both GLUC activity and *E. coli* concentrations varied seasonally (Fig. S2). Peak contamination events and the highest GLUC activity amplitudes (Figs. S4–S5) occurred from late fall to early spring, when heavy rainfall and/or snowmelt episodes contributed to the release of partially treated or untreated sewage into the river through WRRF by-passes and CSOs (Table 1). In contrast, GLUC activity and *E. coli* concentrations were comparatively lower during summer, despite high precipitation volumes in 2017 (Fig. 2). This could be due to higher settling rates and/or prolonged exposure to a combination of biotic (grazing) and abiotic (solar irradiation, temperature) stressors (Blaustein et al., 2013; Servais et al., 2009; Wanjugi and Harwood, 2013) given the longer residence times in the river (Fig. 8). In contrast, during high river flow rates in winter and early spring, dispersion rates increased (Jalliffier-Verne et al., 2017). In addition, the UV-mediated inactivation of *E. coli* at the WRRF could have been suboptimal due to higher particle loads in the primary effluent and lower contact times during disinfection (Örmeci and Linden, 2002). As shown in Fig. 2, lowest UV doses at the WRRF effluent were measured during winter and early spring.

At shorter time scales, we identified three weather patterns that triggered GLUC activity peaks of different magnitudes and durations at the DWTP intake: 1) intense ($\geq$30 $mm.day^{-1}$) precipitation, 2) snowmelt, 3) precipitation (>10 $mm.day^{-1}$) during snowmelt. Snowmelt episodes caused progressive GLUC activity increases and those contamination events lasted for several days (Fig. 5). In contrast, intense precipitation events caused steeper and shorter GLUC activity peaks, the magnitude of which depended on the river flow rate. For instance, intense precipitation on Dec 2, 2016 (Fig. S4) triggered the highest recorded GLUC activity peak (>55

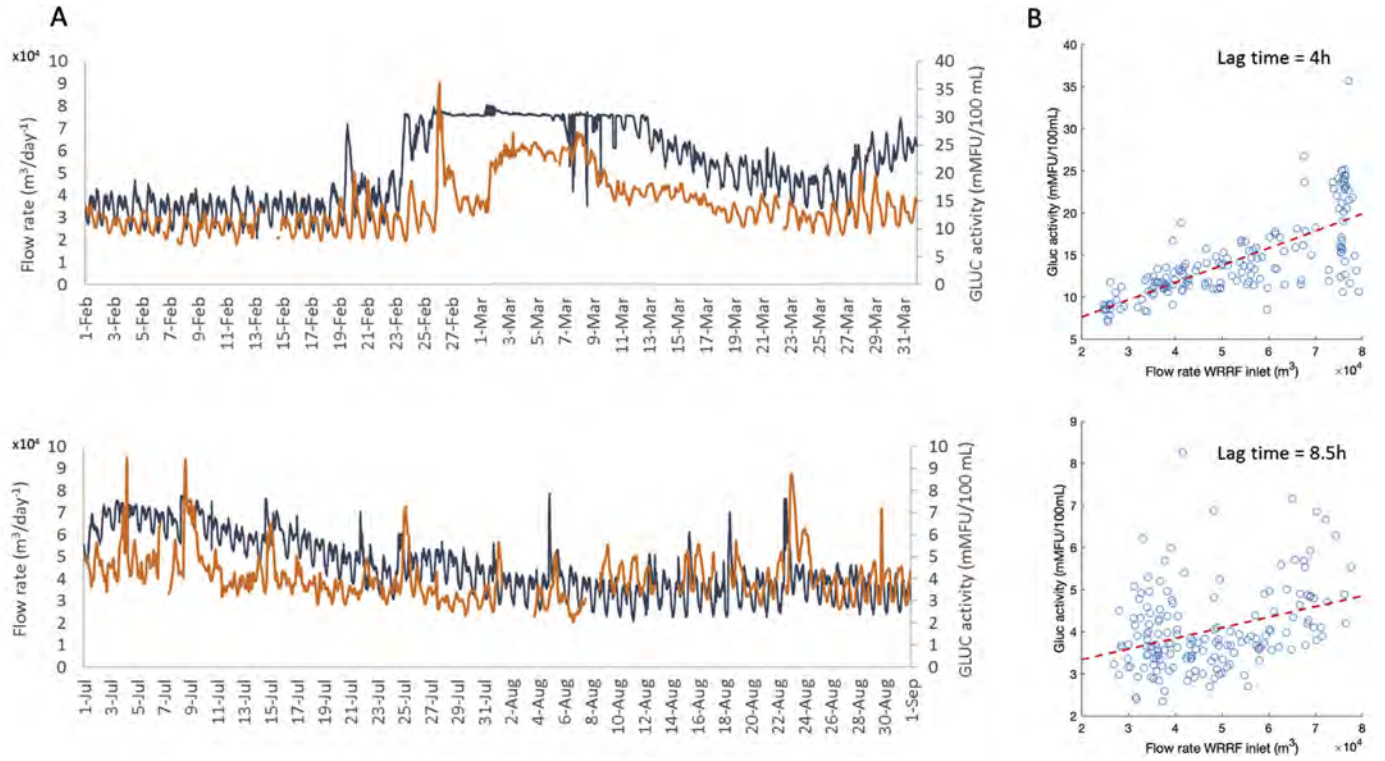

Fig. 6. Cross-correlation between raw sewage flow rate measured at the upstream WRRF and online GLUC activity measured at the DWTP intake a) time series of GLUC activity (orange) and flow rate in raw sewage (black) representative of winter (February to March 2017) and summer (July to August 2017) conditions. A lag time of 4 h in winter and of 8.5 h in summer maximizes the similarity of the time series b) Upper panel: linear regression between the lagged WRRF time series and the DWTP time series in winter ($p < 0.001$ and $R^2 = 0.53$). Lower panel: linear regression between the lagged WRRF time series and the DWTP time series in summer ($p < 0.001$ and $R^2 = 0.12$). (For interpretation of the references to color in this figure legend, the reader is referred to the Web version of this article.)

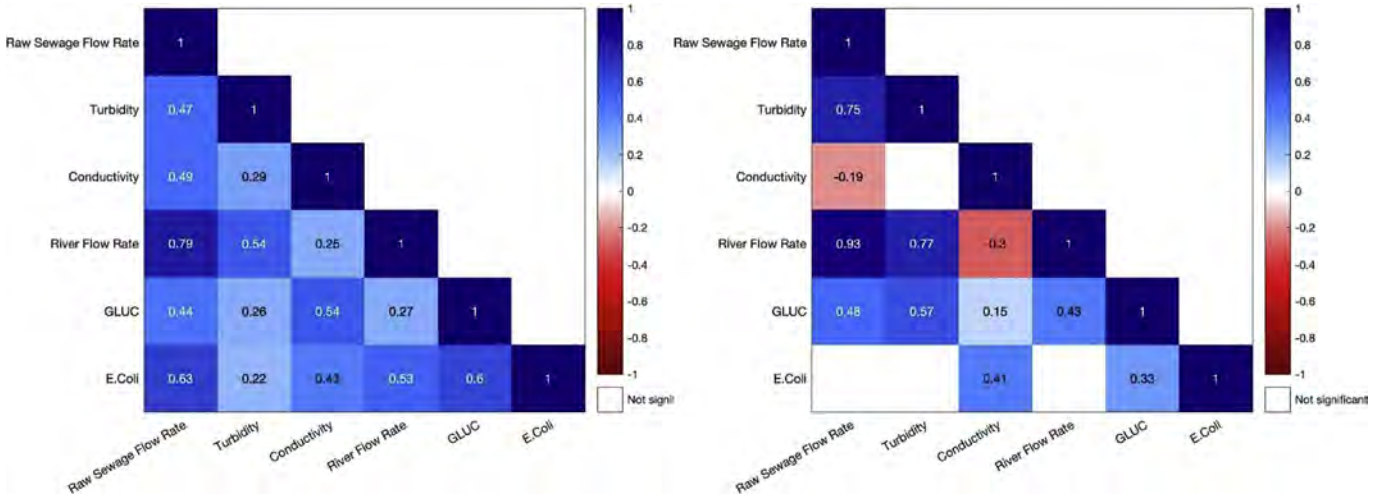

Fig. 7. Correlation matrices for online parameters measured in this study. a) "high GLUC activity" period, b) "low GLUC activity" period (see material and methods section). The blank cells are the ones for which the correlation coefficient was not significant at the $\alpha = 1/20$ level. Note that all the colored cells are significant at the $\alpha = 1/1000$ level.

mMFU.100 mL^{-1}), likely due to limited dilution in the river under unusually low flow rate conditions (Fig. S3c). Following a precipitation event of similar intensity on June 6, 2018, GLUC activity peaked only at 10 mMFU.100 mL^{-1} (Fig. S5). Historically high river flow rates were recorded at that time of the year, following the worst spring floods in the region since 1976. The latter occurred in May 2017 and resulted from a combination of a relatively deep snowpack, saturated soils, and precipitation (OURANOS, 2019) with river flow rates exceeding 1,000 $m^3 s^{-1}$ (1981–2016 average of 380 $m^3 s^{-1}$ for May). The floodwaters were related to regional scale hydrology; they were thus not associated with major and episodic GLUC activity peaks. Despite the occurrences of emergency sewage by-passes throughout the 2017 spring flood, their effect on peak and average GLUC activities progressively diminished (Figs. 2 and 4) due to increased dilution by floodwaters.

Snowmelt and intense precipitation have been shown to cause large increases in *E. coli* concentrations in surface waters (Kistemann et al., 2002; Tornevi et al., 2014; Whitman et al., 2008),

Table 1
Hydrometeorological triggers of GLUC activity peaks (>95th percentile) at the drinking water intake.

Hydro-meteorological triggers	GLUC activity peak		Cumulative rainfall[a]			Max snow cover (cm)	WRRF by-passes (yes/no)	Number of CSO events (outfall #)[b]
	Date	Peak activity (mMFU.100 mL^{-1})	72 h	48 h	24 h			
Rainfall[c]	Dec 2, 2016	55.6	41.3	29.8	1.2		Y	
	Oct 30, 2017	36.9	35.6	35.6	11.1		Y	
	April 5, 2018	29.4	29.7	29.7	0		Y	2 (5,13)
Snowmelt[d]	Mar 3, 2018	46.1				29.0	Y	
Rainfall + snowmelt	Dec 27, 2016	39.8	24.8	13.5	13.5	15.0	N	
	Jan 12, 2017	30.4	32.7	32.7	32.7	9.0	N	1 (9)
	Feb 26, 2017	36.0	27.2	26.5	22.9	29.0	Y	1 (17)
	April 5, 2017	35.9	40.2	39.3	39.3	28.0	Y	2 (6,9)
	Jan 12, 2018	29.4	50.1	50.1	38.0	16.0	Y	
	Jan 21, 2018	39.6	12.1	12.1	12.1	21.0	Y	1 (9)

[a] Time before peak GLUC activity.
[b] For CSOs within the intake intermediary protection zone (discharge points 6–22, see Fig. 1).
[c] Absence of snow melt at least 3 days prior to the GLUC activity peak event.
[d] 3 days-cumulated rainfall <1 mm.

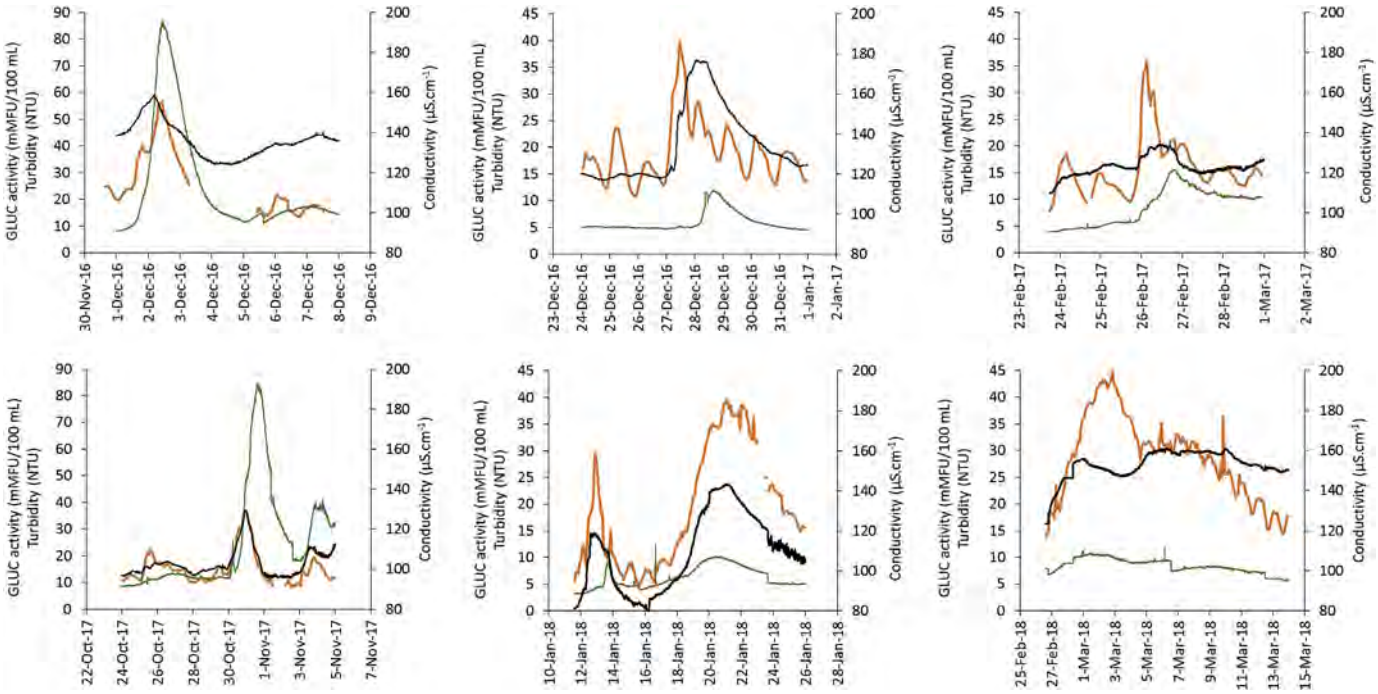

Fig. 8. Relationship between times series for online GLUC activity (orange), turbidity (green) and conductivity (black) following intense precipitation and/or snowmelt episodes (see Table 1 for details). (For interpretation of the references to color in this figure legend, the reader is referred to the Web version of this article.)

which was also observed in our settings. In addition, the use of near real-time monitoring of GLUC activity enabled a more thorough characterization of the frequency, magnitude and duration of episodic microbial spikes at the intake under a series of hydro-meteorological conditions, some of which were historic for the region. The availability of online monitoring during the 2017 flood was reassuring for water managers given that it provided real-time data during an emergency. Such information is important for the identification of upstream pollution sources and for better appraisal of the timing and magnitude of hazardous events in the drinking water supply towards improved human health protection (WHO, 2016).

4.4. Online β-D-glucuronidase monitoring as early warning fecal indicator?

Besides recent technologies for near real-time monitoring of microbial parameters such as the one used in this study, online sensors for turbidity and conductivity provide rapid and automated high frequency measurements. They are routinely used by water utilities for real-time monitoring of source water quality and water treatment processes. Recent studies though have reported the absence or weak association between these parameters and GLUC activity (Stadler et al., 2016; Ender et al., 2017; Ryzinska-Paier et al., 2014; Stadler et al., 2010). Our results show that the relationship

between online GLUC activity and turbidity depended on the period of the year. It was moderate ($r = 0.57$) during the "low GLUC activity" period (late spring to end of summer) but much weaker during the "high GLUC activity" period (fall to early spring) (Fig. 7). During the latter period, a lag of 18 to >24 h was observed between most GLUC activity and turbidity peaks (Fig. 8). Furthermore, online turbidity did not reflect daily patterns as those reported by GLUC activity. Conductivity can be indicative of point sources of fecal pollution such as WRRFs (De Sousa et al., 2014) and its strong relationship with GLUC activity during the "high GLUC activity" period (Fig. 7) confirmed the impact of WRRF effluents on the drinking water intake. Ort and Siegrist (2009) reported daily conductivity fluctuations in a small creek, which were associated with discharge variations from an upstream WRRF. In this study, we observed daily conductivity variations, but their amplitude was much lower than for GLUC activity. Furthermore, during local snowmelt isolated conductivity peaks possibly caused riverine inputs of road salt were observed in absence of GLUC activity peaks (Fig. S6). During the February 2017 event, online conductivity and turbidity values increased over time, but their respective peaks were delayed by several hours compared to GLUC activity (Fig. 8). Considering that *E. coli* concentrations quickly rose by > 1 $\log_{10}$ along the GLUC activity peak (Fig. 4), reliance on conductivity or turbidity would thus have led to the omission of this episodic fecal pollution spike at the intake.

Significant relationships between GLUC activity and culturable *E. coli* have been reported previously, especially during contamination peaks (Burnet et al., 2019; Ender et al., 2017; Stadler et al., 2016, 2019b). Based on routine and event-based monitoring, *E. coli* concentrations associated with GLUC activities >95th percentile (>27.7 mMFU.100 mL^{-1}) ranged from 108 to 2,720 CFU.100 mL^{-1}. This variability in *E. coli* concentrations during GLUC activity peaks may have resulted from contrasting compositions in *E. coli* populations in terms of metabolic status (Garcia-Armisen et al., 2005). In winter and spring, *E. coli* concentrations dropped quicker than GLUC activities following snowmelt-driven contamination peaks (Fig. 4). Given that culturable *E. coli* rapidly decline in snow but may remain viable for weeks (Staley et al., 2017), snowmelt runoff could have carried a large proportion of non-culturable, yet GLUC active *E. coli* cells that contributed to the enzymatic signal. In contrast, synchronous rapid increases in GLUC activity and *E. coli* following intense precipitation strongly suggested the transport of recent contamination from local sewage discharges. Online GLUC activity could thus be used as early warning tool for the detection of episodic fecal contamination peaks in the drinking water supply.

Additional research is needed to better understand the potential sources and sinks of non-target microorganisms and their effect on GLUC activity measurements (Fiksdal and Tryland, 2008). The contribution of river sediment resuspension on the mobilization of GLUC active microorganisms, especially during runoff conditions (Stadler et al., 2019b) also warrants further investigations. Finally, data on the persistence of GLUC signals in comparison to culturable *E. coli* are needed to determine their respective fate and transport in water. This knowledge will provide insights into the applicability of online GLUC activity as fecal indicator and early warning system in diverse aquatic environments.

4.5. Advancing water quality monitoring frameworks using online near real-time measurement of GLUC activity

Compliance monitoring frameworks have been inadequate in preventing waterborne disease outbreaks and ensuring safe drinking water supply in developed nations, notably because of suboptimal monitoring strategies (Hrudey et al., 2003). The latter do not reliably describe source water quality fluctuations, which can influence microbial risk. These fluctuations are directly associated with hydrometeorological factors such as intense precipitation and spring snowmelt that have led to major waterborne disease outbreaks within the past three decades (Curriero et al., 2001; Thomas et al., 2006).

Even though routine monitoring of *E. coli* in source water occurred more frequently at the studied DWTP than the prescribed weekly sampling, most *E. coli* peak concentrations were missed in absence of targeted sample collection (Figs. 2 and 4). As source water protection aims to reduce peak concentrations, the representativeness of source water monitoring should be improved by also explicitly targeting peak concentration events. We show that near real-time monitoring of GLUC activity enabled to characterize the frequency, duration and magnitude of contamination peaks and provided crucial knowledge on the nature and timing of upstream pollution sources affecting the DWTP intake under baseline and event conditions. Near-real time online information by GLUC activity time series will further offer new opportunities for targeted sampling of additional water quality parameters (Ryzinska-Paier et al., 2014).

Ongoing work aims at assessing the relationships between GLUC activity, culturable *E. coli* and the occurrence of waterborne pathogens and fecal source markers under various hydrometeorological settings. Such data will eventually help assessing the value of online GLUC activity in microbial risk assessment and fecal source tracking to help water utilities better track critical situations in their water supply. In a context of growing vulnerability of drinking water supplies to global changes, source mitigation measures could be better prioritized to efficiently reduce the fecal burden upstream of the drinking water treatment train.

5. Conclusions

- Online monitoring of GLUC activity was performed at bi-hourly frequency for 1.5 years to unravel temporal scales of fecal pollution dynamics at an urban drinking water treatment plant (DWTP) intake.
- GLUC activity displayed seasonal to hourly patterns of temporal fluctuation, peak contamination episodes being observed from late fall to early spring.
- Recurrent daily patterns in GLUC activity provided a fingerprint of a continuous impact of treated wastewater effluents on the microbial water quality at the DWTP intake.
- Peak contamination episodes were triggered by rainfall and/or snowmelt-induced sewage by-passes from an upstream water resources recovery facility (WRRF).
- Combined sewer overflows appeared to have a comparatively lower impact than sewage by-passes because of their distance to the intake and lower discharged volumes.
- The relationships between GLUC activity, *E. coli* and online physico-chemistry varied seasonally; GLUC and *E. coli* peaked synchronously during episodic contamination events.
- Acquisition of high frequency measurement datasets improves our understanding of catchment microbial dynamics through identification and characterization of intermittent pollution peaks in drinking water supplies.

The authors declare no conflict of interest.

Acknowledgements

We would like to acknowledge Denis Allard, Mario Gagné, Claude Durivage, Guy Filiatrault Laurène Autixier, Marianne Dupont and Daphnée Archambault-Martel for their collaboration in this

study. We also thank Yves Fontaine, Tuc Quoc Dinh, Mounia Hachad and Joïa Ceccantini for excellent laboratory and field work assistance. The present study was financially supported by the Canada Research Chair in Source Water Protection and the NSERC Industrial Chair on Drinking Water Treatment and its partners (City of Montreal, City of Laval, City of Longueuil, City of Repentigny, and John Meunier Inc. (Veolia)).

Appendix A. Supplementary data

Supplementary data to this article can be found online at https://doi.org/10.1016/j.watres.2019.114869.

References

Bergmeyer, H.U., 2012. Methods of Enzymatic Analysis. Elsevier.
Besmer, M.D., Weissbrodt, D.G., Kratochvil, B.E., Sigrist, J.A., Weyland, M.S., Hammes, F., 2014. The feasibility of automated online flow cytometry for *In-situ* monitoring of microbial dynamics in aquatic ecosystems. Front. Microbiol. 5, 1–12. https://doi.org/10.3389/fmicb.2014.00265.
Blaustein, R.A., Pachepsky, Y., Hill, R.L., Shelton, D.R., Whelan, G., 2013. *Escherichia coli* survival in waters: temperature dependence. Water Res. 47, 569–578. https://doi.org/10.1016/j.watres.2012.10.027.
Boehm, A.B., 2007. Enterococci concentrations in diverse coastal environments exhibit extreme variability. Environ. Sci. Technol. 41, 8227–8232. https://doi.org/10.1021/es071807v.
Burnet, J.-B., Penny, C., Ogorzaly, L., Cauchie, H.-M., 2014. Spatial and temporal distribution of *Cryptosporidium* and *Giardia* in a drinking water resource: implications for monitoring and risk assessment. Sci. Total Environ. 472, 1023–1035. https://doi.org/10.1016/j.scitotenv.2013.10.083.
Burnet, J.B., Dinh, Q.T., Imbeault, S., Servais, P., Dorner, S., Prévost, M., 2019. Autonomous online measurement of β-D-glucuronidase activity in surface water: is it suitable for rapid *E. coli* monitoring? Water Res. 152, 241–250. https://doi.org/10.1016/j.watres.2018.12.060.
Cann, K.F., Thomas, D.R., Salmon, R.L., Wyn-Jones, A.P., Kay, D., 2013. Extreme water-related weather events and waterborne disease. Epidemiol. Infect. 141, 671–686. https://doi.org/10.1017/S0950268812001653.
Chatfield, C., 2003. In: The Analysis of Time Series: an Introduction, sixth ed. Chapman and Hall/CRC.
Curriero, F.C., Patz, J.A., Rose, J.B., Lele, S., 2001. The association between extreme precipitation and waterborne disease outbreaks in the United States, 1948–1994. Am. J. Public Health 91, 1194–1199. https://doi.org/10.2105/AJPH.91.8.1194.
Drewes, J.E., Hübner, U., Zhiteneva, V., Karakurt, S., 2017. Characterization of Unplanned Water Reuse in the EU. Final Report. European Comission DG Environment, pp. 1–61.
Ender, A., Goeppert, N., Grimmeisen, F., Goldscheider, N., 2017. Evaluation of β-D-glucuronidase and particle-size distribution for microbiological water quality monitoring in Northern Vietnam. Sci. Total Environ. 580, 996–1006. https://doi.org/10.1016/j.scitotenv.2016.12.054.
Environment Canada, 2019. Historical Hydrometric Data accessed April 18, 2019. https://eau.ec.gc.ca/mainmenu/historical_data_index_f.html.
Farnleitner, A.H., Hocke, L., Beiwl, C., 2001. Rapid enzymatic detection of *Escherichia coli* contamination in polluted river water. Lett. Appl. Microbiol. 33, 246–250. https://doi.org/10.1046/j.1472-765X.2001.00990.x.
Fiksdal, L., Pommepuy, M., Caprais, M.P., Midttun, I., 1994. Monitoring of fecal pollution in coastal waters by use of rapid enzymatic techniques. Appl. Environ. Microbiol. 60, 1581–1584.
Fiksdal, L., Tryland, I., 2008. Application of rapid enzyme assay techniques for monitoring of microbial water quality. Curr. Opin. Biotechnol. 19, 289–294. https://doi.org/10.1016/j.copbio.2008.03.004.
Garcia-Armisen, T., Lebaron, P., Servais, P., 2005. β-D-glucuronidase activity assay to assess viable *Escherichia coli* abundance in freshwaters. Lett. Appl. Microbiol. 40, 278–282. https://doi.org/10.1111/j.1472-765X.2005.01670.x.
Højris, B., Christensen, S.C.B., Albrechtsen, H.J., Smith, C., Dahlqvist, M., 2016. A novel, optical, on-line bacteria sensor for monitoring drinking water quality. Sci. Rep. 6, 1–10. https://doi.org/10.1038/srep23935.
Hrudey, S.E., Huck, P.M., Payment, P., Gillham, R.W., Hrudey, E.J., 2003. Walkerton : lessons learned in comparison with waterborne outbreaks in the developed world. J. Environ. Eng. Sci. 1, 397–407. https://doi.org/10.1139/S02-031.
IWA, 2019. Abstraction source for water supply. http://waterstatistics.iwa-network.org/graph/2 accessed April 18, 2019.
IWA, 2018. Microbial Sensors for the Drinking Water Industry. International Water Association.
Jalliffier-Verne, I., Leconte, R., Huaringa-Alvarez, U., Heniche, M., Madoux-Humery, A.-S., Autixier, L., Galarneau, M., Servais, P., Prévost, M., Dorner, S., 2017. Modelling the impacts of global change on concentrations of *Escherichia coli* in an urban river. Adv. Water Resour. 108, 450–460. https://doi.org/10.1016/j.advwatres.2016.10.001.
Jalliffier-Verne, I., Servais, P., Galarneau, M., Madoux-Humery, A.-S., Prévost, M., Heniche, M., Dorner, S., 2016. Cumulative effects of fecal contamination from combined sewer overflows: management for source water protection. J. Environ. Manag. 174, 62–70. https://doi.org/10.1016/j.jenvman.2016.03.002.
Jirka, G.H., Bleninger, T., Burrows, R., Larsen, T., 2004. Management of point source discharges into rivers: where do environmental quality standards in the new EC-water framework directive apply? Int. J. River Basin Manag. 2, 225–233. https://doi.org/10.1080/15715124.2004.9635234.
Khan, S.J., Deere, D., Leusch, F.D.L., Humpage, A., Jenkins, M., Cunliffe, D., 2015. Extreme weather events: should drinking water quality management systems adapt to changing risk profiles? Water Res. 85, 124–136. https://doi.org/10.1016/j.watres.2015.08.018.
Kistemann, T., Classen, T., Koch, C., Dangendorf, F., Fischeder, R., Gebel, J., Vacata, V., Exner, M., 2002. Microbial load of drinking water reservoir tributaries during extreme rainfall and runoff. Appl. Environ. Microbiol. 68, 2188–2197. https://doi.org/10.1128/aem.68.5.2188-2197.2002.
Koschelnik, J., Vogl, W., Epp, M., Lackner, M., 2015. Rapid analysis of β-D-glucuronidase activity in water using fully automated technology. Water Resour. Manag. VIII 196, 471–481. https://doi.org/10.2495/WRM150401.
Madoux-Humery, A.-S., Dorner, S.M., Sauvé, S., Aboulfadl, K., Galarneau, M., Servais, P., Prévost, M., 2015. Temporal analysis of *E. coli*, TSS and wastewater micropollutant loads from combined sewer overflows: implications for management. Environ. Sci. Process. Impacts 17, 965–974. https://doi.org/10.1039/c5em00093a.
Madoux-Humery, A.S., Dorner, S., Sauvé, S., Aboulfadl, K., Galarneau, M., Servais, P., Prévost, M., 2016. The effects of combined sewer overflow events on riverine sources of drinking water. Water Res. 92, 218–227. https://doi.org/10.1016/j.watres.2015.12.033.
Madrid, Y., Zayas, Z.P., 2007. Water sampling: traditional methods and new approaches in water sampling strategy. Trends Anal. Chem. 26, 293–299. https://doi.org/10.1016/j.trac.2007.01.002.
MDDELCC, 2016. Règlement sur le prélèvement des eaux et leur protection. Quebec Ministry of Environment.
Örmeci, B., Linden, K.G., 2002. Comparison of UV and chlorine inactivation of particle and non-particle associated coliform. Water Sci. Technol. Water Supply 2, 403–410. https://doi.org/10.2166/ws.2002.0197.
Ort, C., Siegrist, H., 2009. Assessing wastewater dilution in small rivers with high resolution conductivity probes. Water Sci. Technol. 59, 1593–1601. https://doi.org/10.2166/wst.2009.174.
Ouattara, N.K., Garcia-Armisen, T., Anzil, A., Brion, N., Servais, P., 2014. Impact of wastewater release on the faecal contamination of a small urban river: the Zenne River in Brussels (Belgium). Water. Air. Soil Pollut. 225, 1–12. https://doi.org/10.1007/s11270-014-2043-5.
OURANOS, 2019. Inondations Mai 2017. https://www.ouranos.ca/questions-reponses-inondations-mai-2017/. accessed April 18, 2019.
Page, R.M., Besmer, M.D., Epting, J., Sigrist, J.A., Hammes, F., Huggenberger, P., 2017. Online analysis: deeper insights into water quality dynamics in spring water. Sci. Total Environ. 599–600, 227–236. https://doi.org/10.1016/j.scitotenv.2017.04.204.
Rice, J., Wutich, A., Westerho, P., 2013. Assessment of *de facto* wastewater reuse across the U.S.: trends between 1980 and 2008. Environ. Sci. Technol. 47, 11099–11105. https://doi.org/10.1021/es402792s.
Ryzinska-Paier, G., Lendenfeld, T., Correa, K., Stadler, P., Blaschke, A.P., Mach, R.L., Stadler, H., Kirschner, A.K.T., Farnleitner, A.H., 2014. A sensitive and robust method for automated on-line monitoring of enzymatic activities in water and water resources. Water Sci. Technol. 69, 1349–1358. https://doi.org/10.2166/wst.2014.032.
Servais, P., Prats, J., Passerat, J., Garcia-Armisen, T., 2009. Abundance of culturable versus viable *Escherichia coli* in freshwater. Can. J. Microbiol. 55, 905–909. https://doi.org/10.1139/W09-043.
Signor, R.S., Ashbolt, N.J., 2006. Pathogen monitoring offers questionable protection against drinking-water risks: a QMRA (Quantitative Microbial Risk Analysis) approach to assess management strategies. Water Sci. Technol. 54, 261–268. https://doi.org/10.2166/wst.2006.478.
Sorensen, J.P.R., Lapworth, D.J., Read, D.S., Nkhuwa, D.C.W., Bell, R.A., Chibesa, M., Chirwa, M., Kabika, J., Liemisa, M., Pedley, S., 2015. Tracing enteric pathogen contamination in sub-Saharan African groundwater. Sci. Total Environ. 538, 888–895. https://doi.org/10.1016/j.scitotenv.2015.08.119.
Stadler, H., Skritek, P., Sommer, R., Mach, R.L., Zerobin, W., Farnleitner, A.H., 2008. Microbiological monitoring and automated event sampling at karst springs using LEO-satellites. Water Sci. Technol. 58, 899–909. https://doi.org/10.2166/wst.2008.442.
Stadler, P., Blöschl, G., Vogl, W., Koschelnik, J., Epp, M., Lackner, M., Oismüller, M., Kumpan, M., Nemeth, L., Strauss, P., Sommer, R., Ryzinska-Paier, G., Farnleitner, A.H., Zessner, M., 2016. Real-time monitoring of beta-d-glucuronidase activity in sediment laden streams: a comparison of prototypes. Water Res. 101, 252–261. https://doi.org/10.1016/j.watres.2016.05.072.
Staley, Z.R., He, D.D., Edge, T.A., 2017. Persistence of fecal contamination and pathogenic *Escherichia coli* O157:H7 in snow and snowmelt. J. Great Lakes Res. 43, 248–254. https://doi.org/10.1016/j.jglr.2017.01.006.
Stadler, P., Loken, L., Crawford, J., Schramm, P., Sorsa, K., Kuhn, C., Savio, D., Striegl, R., Butman, D., Stanley, E., Farnleitner, A., Zessner, M., 2019a. Spatial patterns of enzymatic activity in large water bodies: Ship-borne measurements of beta-D-glucuronidase activity as a rapid indicator of microbial water quality. Sci. Tot. Environ. 652, 1742–1752. https://doi.org/10.1016/j.scitotenv.2018.10.084.

Stadler, P., Blöschl, G., Nemeth, L., Oismüller, M., Kumpan, M., Krampe, J., Farnleitner, A., Zessner, M., 2019b. Event-transport of beta-d-glucuronidase in an agricultural headwater stream: assessment of seasonal patterns by on-line enzymatic activity measurements and environmental isotopes. Sci. Tot. Environ. 662, 236–245. https://doi.org/10.1016/j.scitotenv.2019.01.143.

Thomas, M.K., Charron, D.F., Waltner-Toews, D., Schuster, C., Maarouf, A.R., Holt, J.D., 2006. A role of high impact weather events in waterborne disease outbreaks in Canada, 1975-2001. Int. J. Environ. Health Res. 16, 167–180. https://doi.org/10.1080/09603120600641326.

Tolouei, S., Burnet, J.-B., Autixier, L., Taghipour, M., Bonsteel, J., Duy, S.V., Sauvé, S., Prévost, M., Dorner, S., 2019. Temporal variability of parasites, bacterial indicators, and wastewater micropollutants in a water resource recovery facility under various weather conditions. Water Res. 148, 446–458. https://doi.org/10.1016/j.watres.2018.10.068.

Tornevi, A., Bergstedt, O., Forsberg, B., 2014. Precipitation effects on microbial pollution in a river : lag structures and seasonal effect modification. PLoS One 9, e98546. https://doi.org/10.1371/journal.pone.0098546.

Tryland, I., Eregno, F.E., Braathen, H., Khalaf, G., Sjolander, I., Fossum, M., 2015. On-Line monitoring of *Escherichia coli* in raw water at oset drinking water treatment plant, Oslo (Norway). Int. J. Environ. Res. Public Health 12, 1788–1802. https://doi.org/10.3390/ijerph120201788.

USEPA, 2002. Method 1604: Total Coliforms and *Escherichia coli* in Water by Membrane Filtration Using a Simultaneous Detection Technique (MI Medium). United States Environmental Protection Agency, Office of Water.

Wanjugi, P., Harwood, V.J., 2013. The influence of predation and competition on the survival of commensal and pathogenic fecal bacteria in aquatic habitats. Environ. Microbiol. 15, 517–526. https://doi.org/10.1111/j.1462-2920.2012.02877.x.

Weyrauch, P., Matzinger, A., Pawlowsky-Reusing, E., Plume, S., von Seggern, D., Heinzmann, B., Schroeder, K., Rouault, P., 2010. Contribution of combined sewer overflows to trace contaminant loads in urban streams. Water Res. 44, 4451–4462. https://doi.org/10.1016/j.watres.2010.06.011.

Whitman, R.L., Przybyla-Kelly, K., Shively, D.A., Nevers, M.B., Byappanahalli, M.N., 2008. Sunlight, season, snowmelt, storm, and source affect *E. coli* populations in an artificially ponded stream. Sci. Total Environ. 390, 448–455. https://doi.org/10.1016/j.scitotenv.2007.10.014.

WHO, 2017. Climate-resilient Water Safety Plans. World Health Organization.

WHO, 2016. Protecting Surface Water for Health. World Health Organization.

Wilkes, G., Edge, T., Gannon, V., Jokinen, C., Lyautey, E., Medeiros, D., Neumann, N., Ruecker, N., Topp, E., Lapen, D.R., 2009. Seasonal relationships among indicator bacteria, pathogenic bacteria, *Cryptosporidium* oocysts, *Giardia* cysts, and hydrological indices for surface waters within an agricultural landscape. Water Res. 43, 2209–2223. https://doi.org/10.1016/j.watres.2009.01.033.

Young, I., Smith, B.A., Fazil, A., 2015. A systematic review and meta-analysis of the effects of extreme weather events and other weather-related variables on *Cryptosporidium* and *Giardia* in fresh surface waters. J. Water Health 13, 1–17. https://doi.org/10.2166/wh.2014.079.